



# Analysis of the proton background in connection with the calibration of GLAST's calorimeter

S. Incerti, B. Lott, T. Reposeur

## ► To cite this version:

S. Incerti, B. Lott, T. Reposeur. Analysis of the proton background in connection with the calibration of GLAST's calorimeter. 2000, pp.1-16. in2p3-00018228

**HAL Id: in2p3-00018228**

**<https://hal.in2p3.fr/in2p3-00018228>**

Submitted on 1 Jun 2006

**HAL** is a multi-disciplinary open access archive for the deposit and dissemination of scientific research documents, whether they are published or not. The documents may come from teaching and research institutions in France or abroad, or from public or private research centers.

L'archive ouverte pluridisciplinaire **HAL**, est destinée au dépôt et à la diffusion de documents scientifiques de niveau recherche, publiés ou non, émanant des établissements d'enseignement et de recherche français ou étrangers, des laboratoires publics ou privés.

## Analysis of the proton background in connection with the calibration of GLAST's calorimeter

Sébastien Incerti  
Benoît Lott  
Thierry Reposeur  
CENBG

E-mail  
incerti@cenbg.in2p3.fr  
lott@cenbg.in2p3.fr  
reposeur@cenbg.in2p3.fr

### Abstract

Using the Glast simul\_recon simulation package, we estimate the rates of 'multi-mip protons' passing the Level 1 trigger. By making use of the full information supplied by the LAT, we show how this background can be reduced to a negligible level.

# Contents

<b>1</b>	<b>Introduction</b>	<b>3</b>
<b>2</b>	<b>Energy losses</b>	<b>4</b>
2.1	Electromagnetic energy loss . . . . .	4
2.2	Nuclear energy loss . . . . .	4
<b>3</b>	<b>Background rejection</b>	<b>5</b>
3.1	Rejection at the trigger level . . . . .	5
3.2	Off-line ejection . . . . .	6
<b>4</b>	<b>Conclusion</b>	<b>7</b>

# 1 Introduction

The primary calibration of GLAST's calorimeter will be conducted on flight with heavy cosmic-ray nuclei (CNO, Si, Fe), with typical energies greater than a few hundreds MeV/nucleon. For these particles, the electronic energy losses are close to a minimum and are only very weakly energy dependent (these particles are thus referred to as minimum ionizing particles-mips). This latter property will be exploited in the calibration procedure. A large fraction of the dynamic range of the CsI detectors (10 MeV-70 GeV) can be covered by this method. The flux of the heavy nuclei impinging on the entrance face of telescope will be quite low, around a few Hz, while that of protons will be almost 3 orders of magnitude greater (see next section). Because of the nuclear reactions they induce in the materials of the telescope, some of the far more abundant protons may generate signals comparable to those of the heavy nuclei of interest. If not properly discriminated, this pollution may corrupt the calibration. This background must already be rejected at the trigger level as much as possible, so as not to take an excessive toll on the downlink resources. In order to pass the Level 1 Trigger (see below for a recall of the required conditions), the background protons must leave an energy loss in the ACD tiles significantly greater than the minimum-ionisation energy loss. Accordingly, they will be referred to as 'multimip protons' in the following.

We have investigated this background problem by means of the GlastSim simulation. This note describes our results and presents our propositions to reject this contribution both at the trigger level and in the off-line analysis. It will be shown that it can be brought down to a negligible level ( $< 10^{-3}$ ) by making use of the full information provided by the ACD, the tracker and the calorimeter itself.

The GlastSim simulation provides the Monte-Carlo time, so the proton flux can be directly computed. Our data set consists of a proton sample (194603 protons that went through the LAT, corresponding to a time of 67s in orbit) obtained from the chime package of sr\_program and distributed over a  $4\pi$  solid angle. As mentioned in the description of the CHIMESpectrum Class in GlastSim, we keep only protons with an energy (MC\_Energy) less than 100 GeV. The proton flux amounts to 730 Hz for the protons entering the telescope through its front face. Using the relative abundance given in the Review of Particles Physics, p. 151, at 10.6 GeV/nucleon (almost independent of the energy) one obtains the following fluxes for the CR heavy-nuclei: 40 Hz for He, 1.5 Hz for C or O, 0.15 Hz for Fe. These values are compatible with those quoted by J.E. Grove in Ref. [2] for the entire ACD.

The conditions for accepting a CR nucleus for the calorimeter calibration are listed below:

- a single ACD tile firing, with a Veto energy exceeding a given threshold;
- a single trajectory (2 tracks, X and Y, as defined in GlastSim) observed by the Tracker;
- one CsI crystal hit per layer with no glancing: 8 crystals in total;
- no nuclear reactions in the calorimeter.

The last condition can be ascertained by inspecting the relative energy losses in the different CsI layers, which are uniquely defined in the case of electronic stopping power for a given incident energy if there are no Z-changing reactions \*. For heavy nuclei, most nuclei

---

\*A-changing reactions will be more difficult to detect, since for the spallation reactions involved, the velocities of the projectile-like reactions products are very close to that of the projectile. The electronic

Table 1: Nuclei masses and charges.

Particle	Mass $A$	Charge $Z$
C	12	6
O	16	8
Si	28	14
Fe	56	6
Cs	133	55
I	127	53
C	12	6

(> 75% for Fe) will be lost due these reactions associated with an interaction length (12.5 cm for Fe in CsI) comparable to the calorimeter thickness.

## 2 Energy losses

### 2.1 Electromagnetic energy loss

The electromagnetic energy losses have been computed using the Bethe and Bloch formula [1].

The ACD and calorimeter densities along the LAT  $z$  axis are respectively set to :

$$\rho dx|_{\text{Veto}-1.0\text{cm}} = 1.032\text{gcm}^{-2} \quad (1)$$

$$\rho dx|_{\text{Cal}-2.1\text{cm}} = 9.513\text{gcm}^{-2} \quad (2)$$

We can estimate the kinetic energy loss of the dominant nuclei in an ACD tile or in a CsI block. The results are given in Table 2 and illustrated in Figs. 1- 3.

### 2.2 Nuclear energy loss

As mentioned above, protons will also induce nuclear reactions within the detectors and in some special cases, leave a signature similar to those of 'accepted' CR nuclei. The reaction probabilities for a p traversing GLAST parallel to the main axis are 1.4% in the ACD tile, 4% in the tracker Pb foils and 35% in the calorimeter (interaction lengths of 70 cm, 17.1 cm and 36.5 cm for CH, Pb and CsI respectively). By inspecting the parameters MC $_z$ Vertex and MC\_Mat\_Code bearing information of the location of the first interaction, we have identified two main contributions to the multimip protons which may be of concern for the calibration, i.e., associated with large energy deposits both in the ACD and the calorimeter:

---

energy loss depending only on  $\beta$  and  $z$ , the energy loss is unchanged for A-changing reactions.

Table 2: Energy losses in CH and in CsI.

Compound	Particle	Kinetic energy at minimum (GeV)	Energy deposit (GeV)
CH	p	2.30	0.002
CH	He	9.2	0.008
CH	C	27.7	0.075
CH	O	7.0	0.13
CH	Si	64.7	0.40
CH	Fe	128.7	1.40
CsI	p	1.92	0.012
CsI	He	7.8	0.047
CsI	C	23.7	0.43
CsI	O	31.6	0.76
CsI	Si	55.9	2.3
CsI	Fe	112	8.3

- the proton interacts first within the ACD tile, and secondary reactions take place within the calorimeter;

- the first nuclear interaction occurs inside the calorimeter, and some of the reaction products <sup>†</sup> are detected by the ACD, increasing the energy measured by the latter beyond the high-energy threshold.

Fig. 4 displays the yield plotted as functions of the energy measured with the calorimeter,  $E_{\text{Cal}}$  and the energy deposited in the ACD,  $E_{\text{Veto}}$ . The yield associated with  $E_{\text{Veto}} > 75$  MeV and  $E_{\text{Cal}} > 3.4$  GeV, i.e. in the range expected for CR heavy nuclei, is seen to be very significant.

## 3 Background rejection

### 3.1 Rejection at the trigger level

Before addressing the off-line rejection, the situation at the trigger level is examined. Fig. 5 displays the rate of events fulfilling the 'ACD High' trigger condition as a function of the threshold (which should be set significantly lower than the 75 MeV Energy loss expected for C to be on the safe side). For a 20 MeV threshold, the Level 1 trigger rate amounts to 650 Hz and is still greater than 200 Hz for the maximum threshold of 75 MeV. Requiring that only one ACD tile has fired and that the Calorimeter Energy is greater than 2 GeV cuts down the rate to less than 1 Hz. Multimip protons will thus not overwhelm the data acquisition system provided reasonable thresholds are set.

---

<sup>†</sup>probably essentially  $\gamma$ -rays from  $\pi^0$  decay, since charged products,  $\pi^\pm$  would be seen by the tracker.

### 3.2 Off-line ejection

We now turn to the problem of discriminating the CR heavy nuclei against multimip protons. The distribution of the number of CsI crystals with an energy deposit greater than 6 MeV (parameter `CsI_No_Xtals_keep`) is plotted as a function of  $E_{\text{Cal}}$  in Fig. 6, the horizontal scale being blow up so that only the contribution of protons having suffered electronic stopping is visible. As expected, the latter protons are associated with a number of crystals peaking at 8 (see the projection in the inset) and a total energy loss around 96 MeV. The important point to note here is that non-interacting CR nuclei will be associated with a number of crystals of 8, with sometimes one or two more due to tilted trajectories. For a given energy loss in the calorimeter, far more crystals will be hit for multimip protons than for CR nuclei because of the transverse spreading of the many particles produced in the reactions: this difference can be exploited to reject the multimip protons very efficiently.

This behavior of multimip protons is illustrated in Fig. 7 (logarithmic scale), in which the distribution of the crystal number is again plotted as function of  $E_{\text{Cal}}$  (please note the different scale for the latter parameter as compared to Fig. 6) for different conditions (an extra condition on the incident angle with respect to the main axis  $\cos(\theta) < -0.7$  is imposed for all panels except the upper left one). The average number of hit crystals scales roughly linearly with  $E_{\text{Cal}}$ . The average number of hit crystals is 38 for  $E_{\text{Cal}} > 2$  GeV. In Fig. 7, the boxes depict the regions corresponding to non-interacting CR nuclei heavier than C (`CsI_No_Xtals_keep`=8,  $E_{\text{Cal}} > 3.4$  GeV ).

Although no troublesome protons survive once a limit is set on the number of hit crystals, we have nevertheless attempted to estimate the residual background from the simulation. Surmising that the distribution of the number of CsI crystals hit assumes the same gaussian distribution whether or not the cut on the Veto energy deposit is applied, the number of protons associated with less than 10 Crystals can be estimated. Fig. 8 shows the gaussian fit to the number of CsI crystals without the Veto energy cut, for  $E_{\text{Cal}} > 2$  GeV. The integration shows that about 3 events would be associated with fewer than 10 crystals. Applying the Veto energy cut, 18 events are isolated, to be compared to 1667 events obtained without the cut. A rescaled value of  $3 \times 18 / 1667 = 0.03$  event, satisfying all the cuts and associated with fewer than 10 crystals, is obtained, giving a rate close to  $5 \cdot 10^{-4}$  Hz, that is less than 50 events a day, according to this very crude estimate. According to an estimate from J. E. Grove [2], in the case of C, 1100 nuclei passing the cuts are expected to be recorded for a single Crystal per day. This figure corresponds to  $2.1 \cdot 10^5$  events a day for the LAT, since the calorimeter contains 1536 blocks and 8 crystals are hit for these events. The contamination in 'C like' protons is consequently in the one-per-mille range (note that we have applied only very loose cuts on the energy parameters).

This contamination can be even further reduced by applying cuts on the ratio of measured energies for two consecutive layers. For instance, a very conservative cuts of  $1 \pm 0.15$  on this ratio for the first two layers allows the rejection of more than 80% of the background (Fig. 9). How much of this rejection potential remains once the cut on the number of hit crystals has been applied is hard to estimate without a simulation with much more statistics. Nevertheless, this degree of freedom carries some significant rejection power and can be exploited if necessary.

## 4 Conclusion

We can safely conclude that the multimip protons can be rejected to a negligible level thanks to the wealth of information provided by the LAT. This conclusion is very likely to hold also for He, although no simulation has been performed for the latter: it is indeed well established that nuclear reactions induced by p and He are very similar when compared at the same total bombarding energy, provided the latter is greater than 5 GeV.

## References

- [1] Particle Physics Booklet, p. 189 (2000).
- [2] Calibration with cosmic rays, Glast software meeting, p. 49, 6-8 Sept 2000.



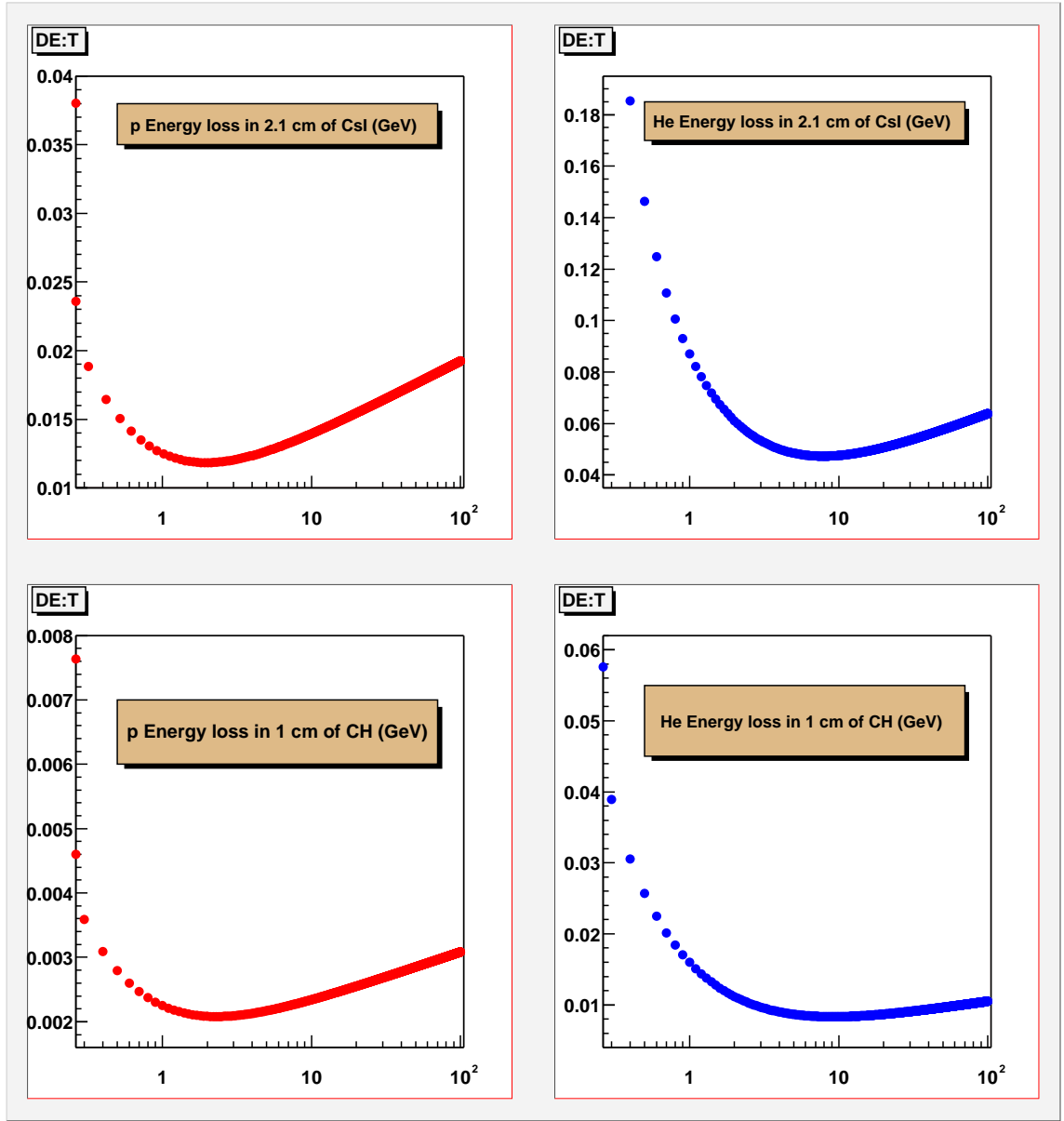


Figure 1: p and He total energy losses (GeV) in CH and in CsI as a function of the bombarding energy (GeV).

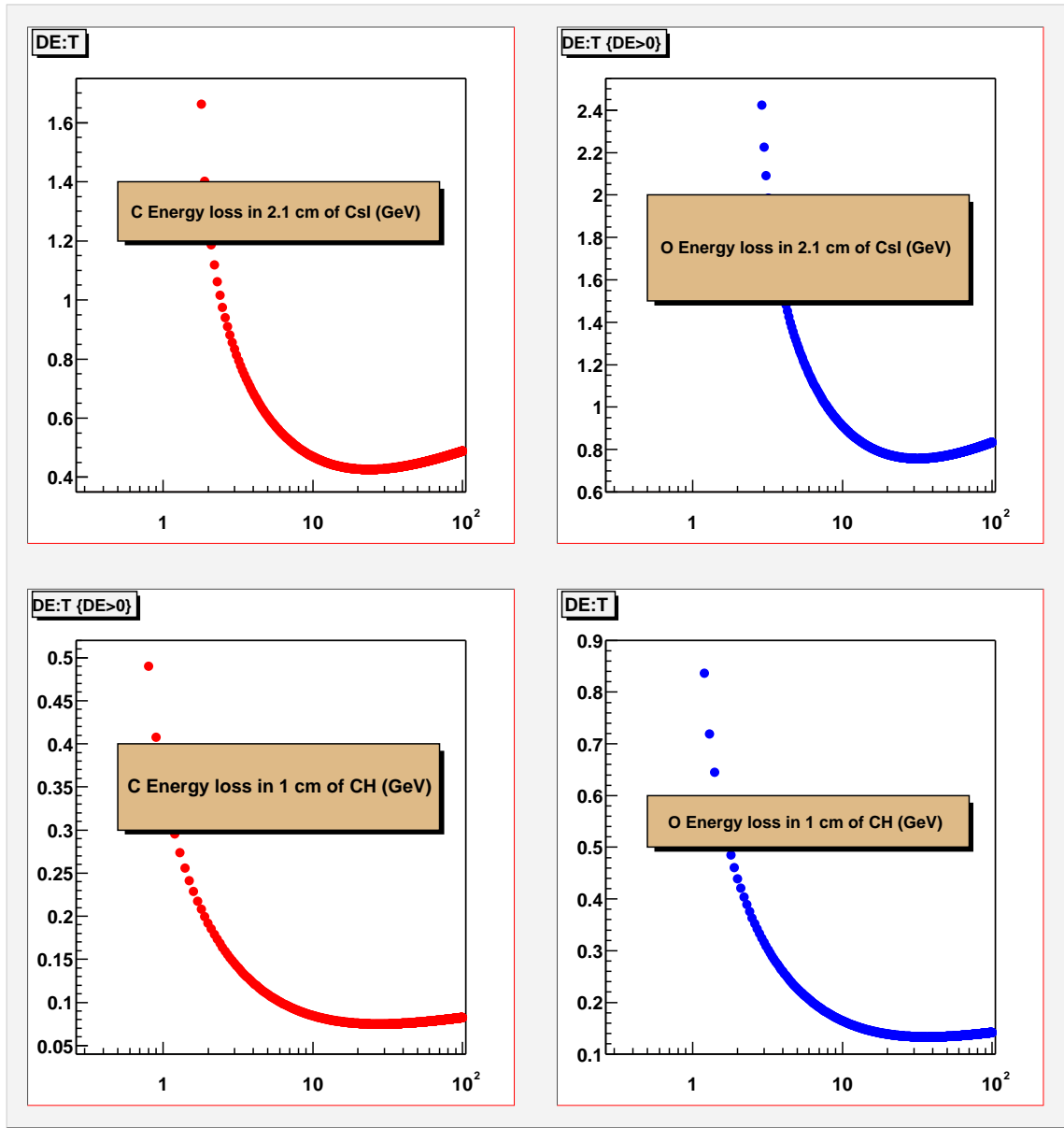


Figure 2: C and O total energy losses (GeV) in CH and in CsI as a function of the bombarding energy (GeV).

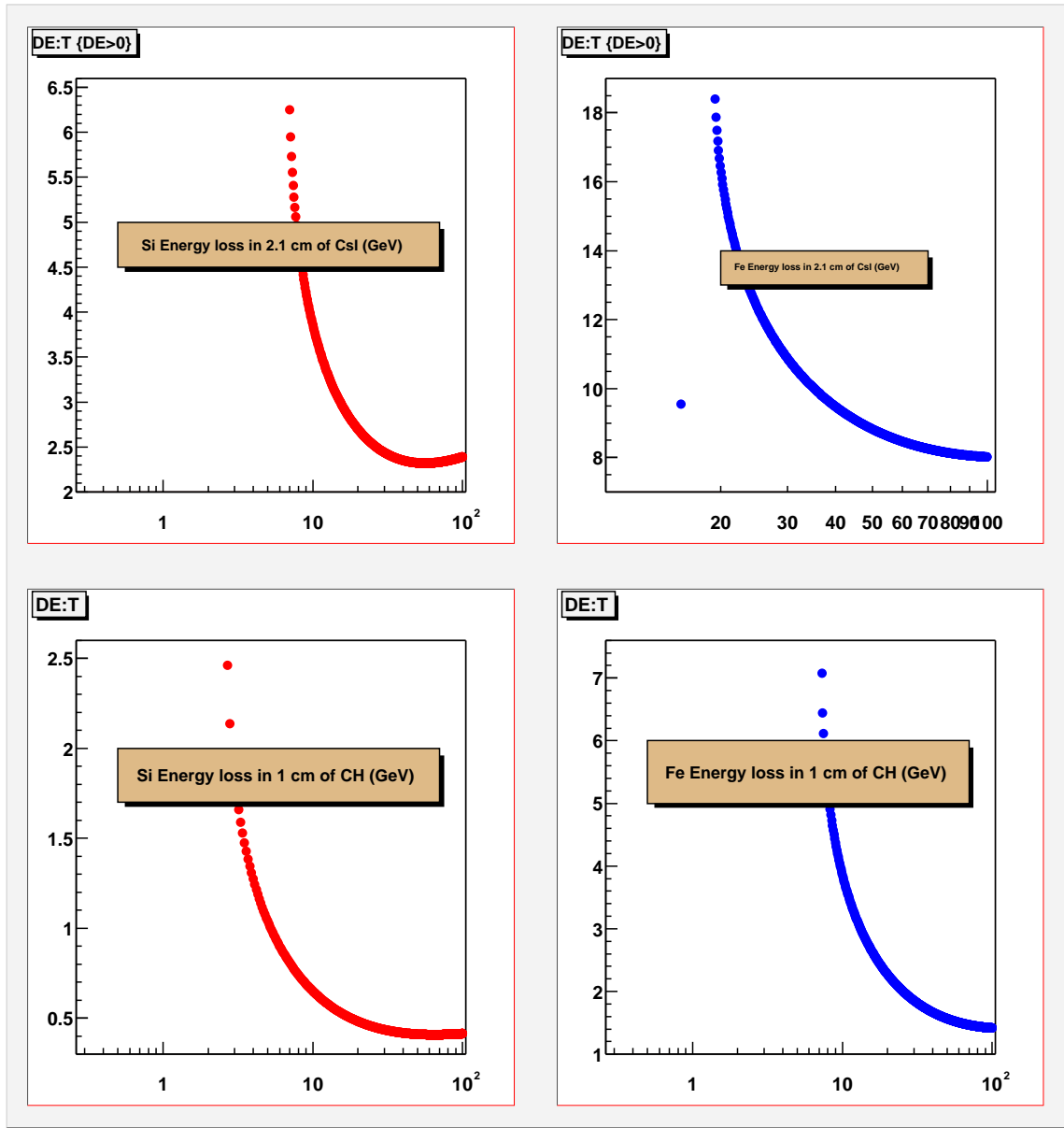


Figure 3: Si and Fe total energy losses (GeV) in CH and in CsI as a function of the bombarding energy (GeV).

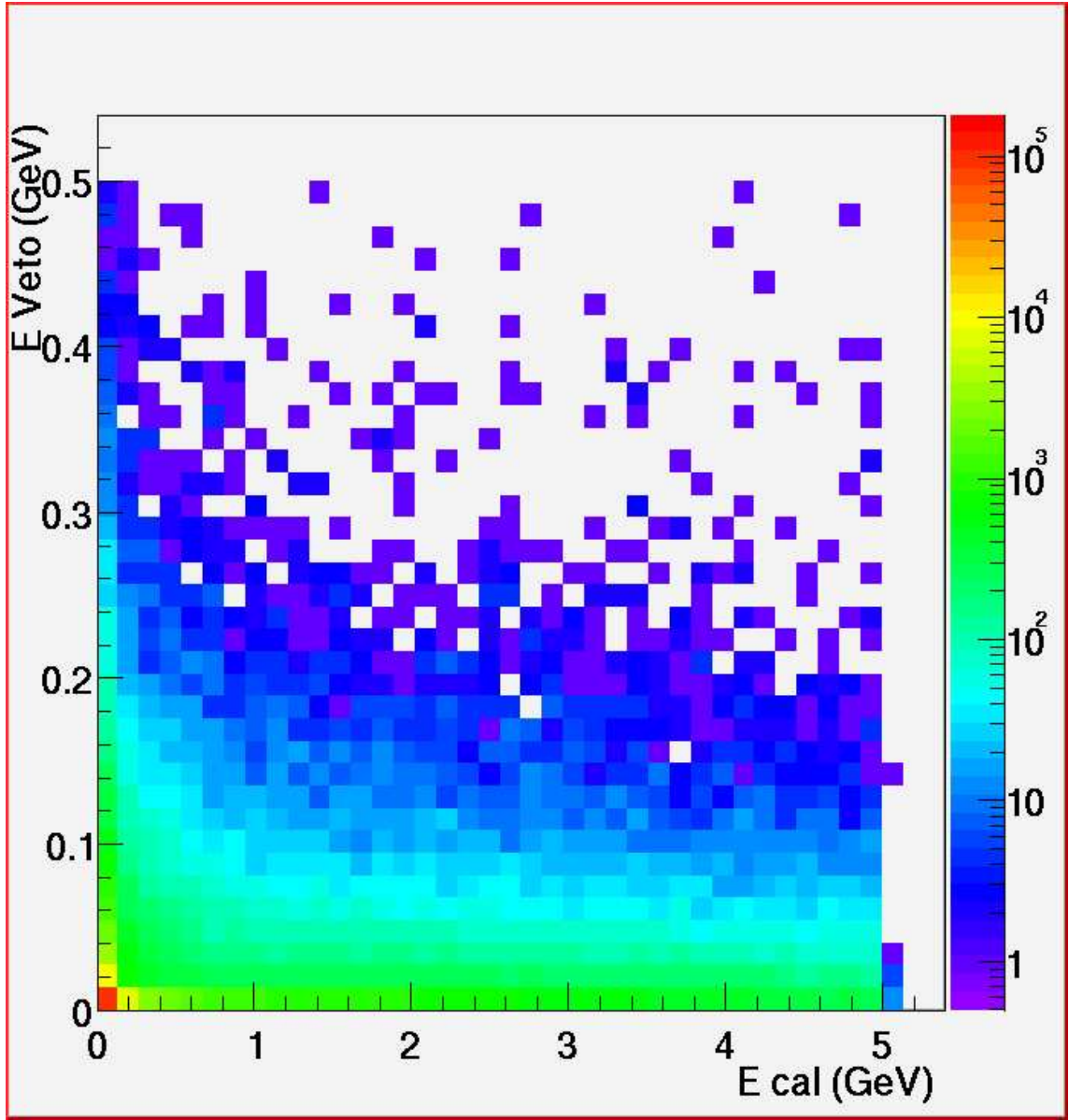


Figure 4: Yield plotted as functions of the energy left in the calorimeter and the energy deposited in the ACD.

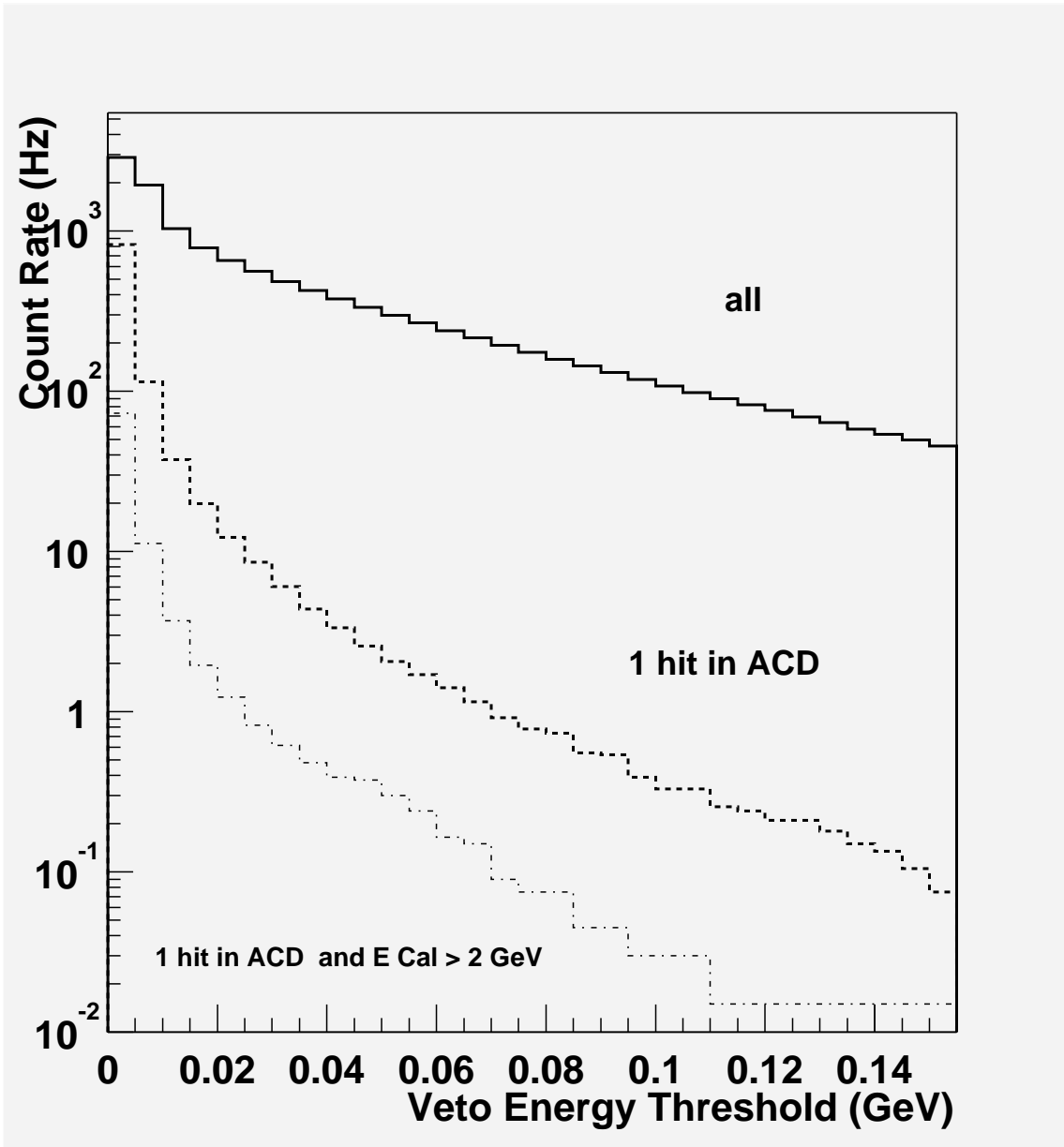


Figure 5: Count rate of events as a function of the ACD energy threshold.

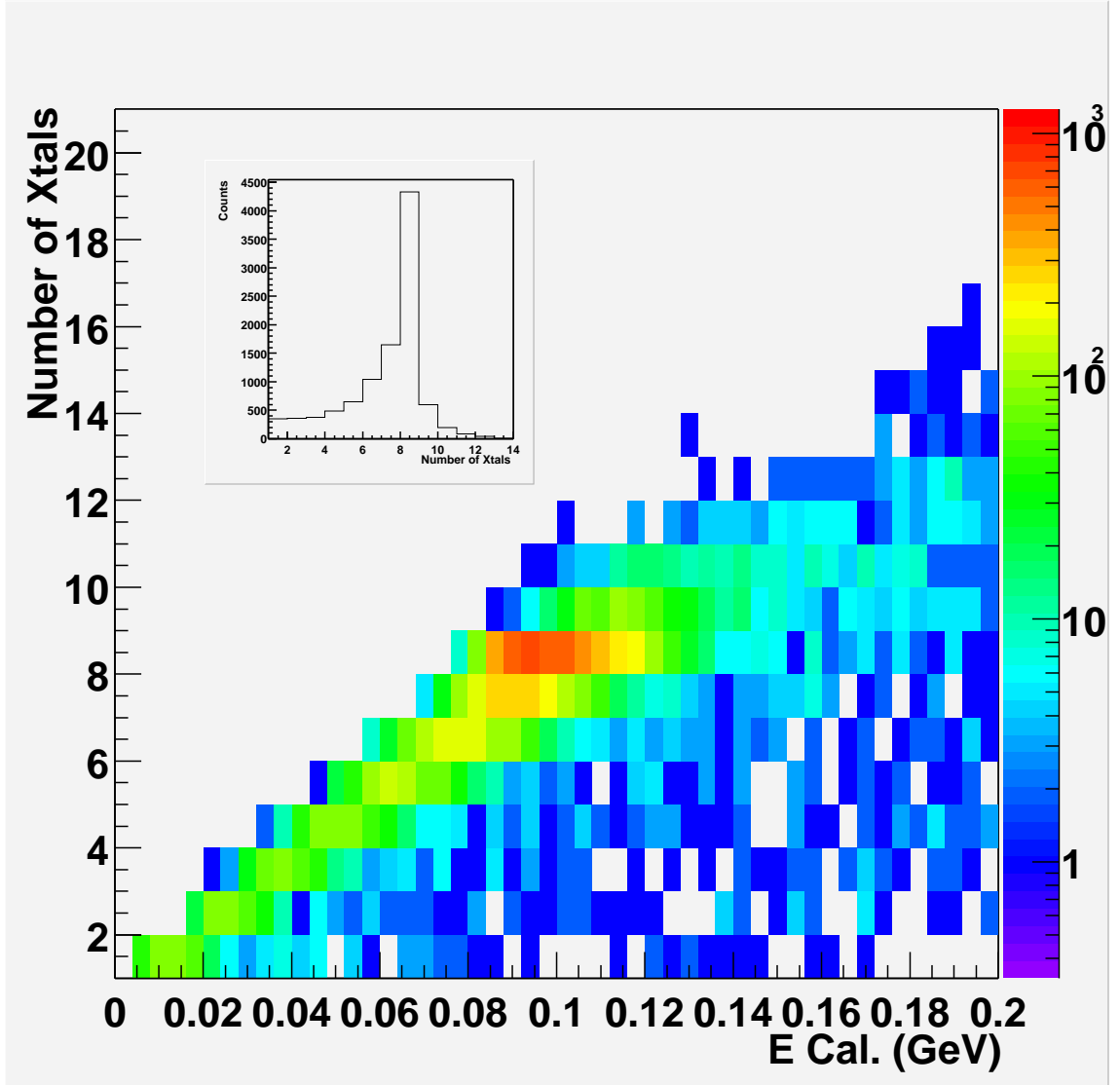


Figure 6: Distribution of the number of CsI crystals with an energy deposit greater than 6 MeV as a function of the energy deposited in the calorimeter. The inset displays the integrated distribution for events with  $E_{\text{Cal}} < 200$  MeV

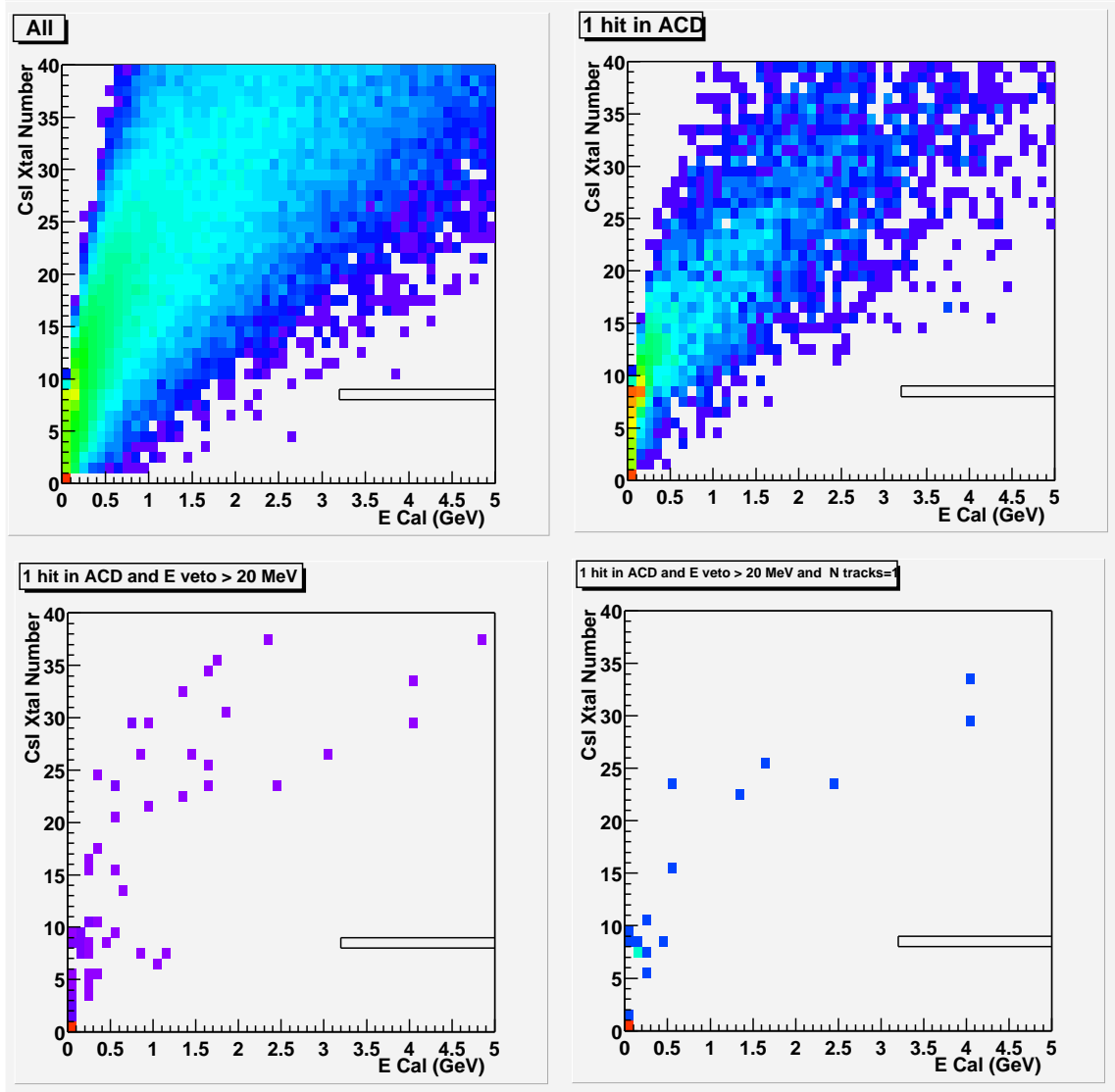


Figure 7: Same as the previous figure, for a different E Cal range. The rectangles depict the region corresponding to the CR nuclei used for the calorimeter calibration.

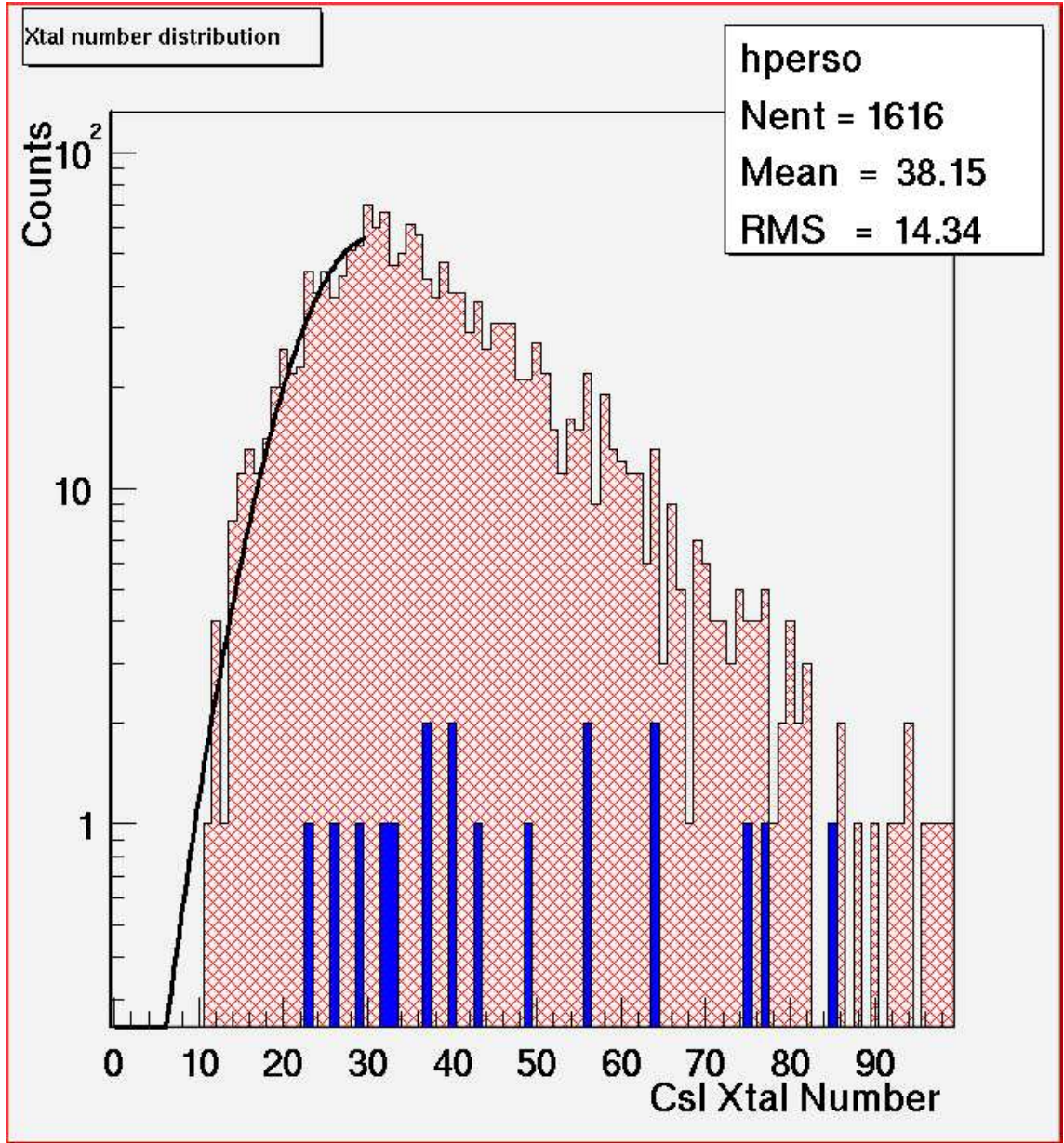


Figure 8: Distribution of the number of CsI crystals with an energy deposit greater than 6 MeV for events associated with one hit in the ACD (hatched) and for the same with the additional condition  $EVeto > 20$  MeV (solid). The line corresponds to the gaussian fit described in the text.



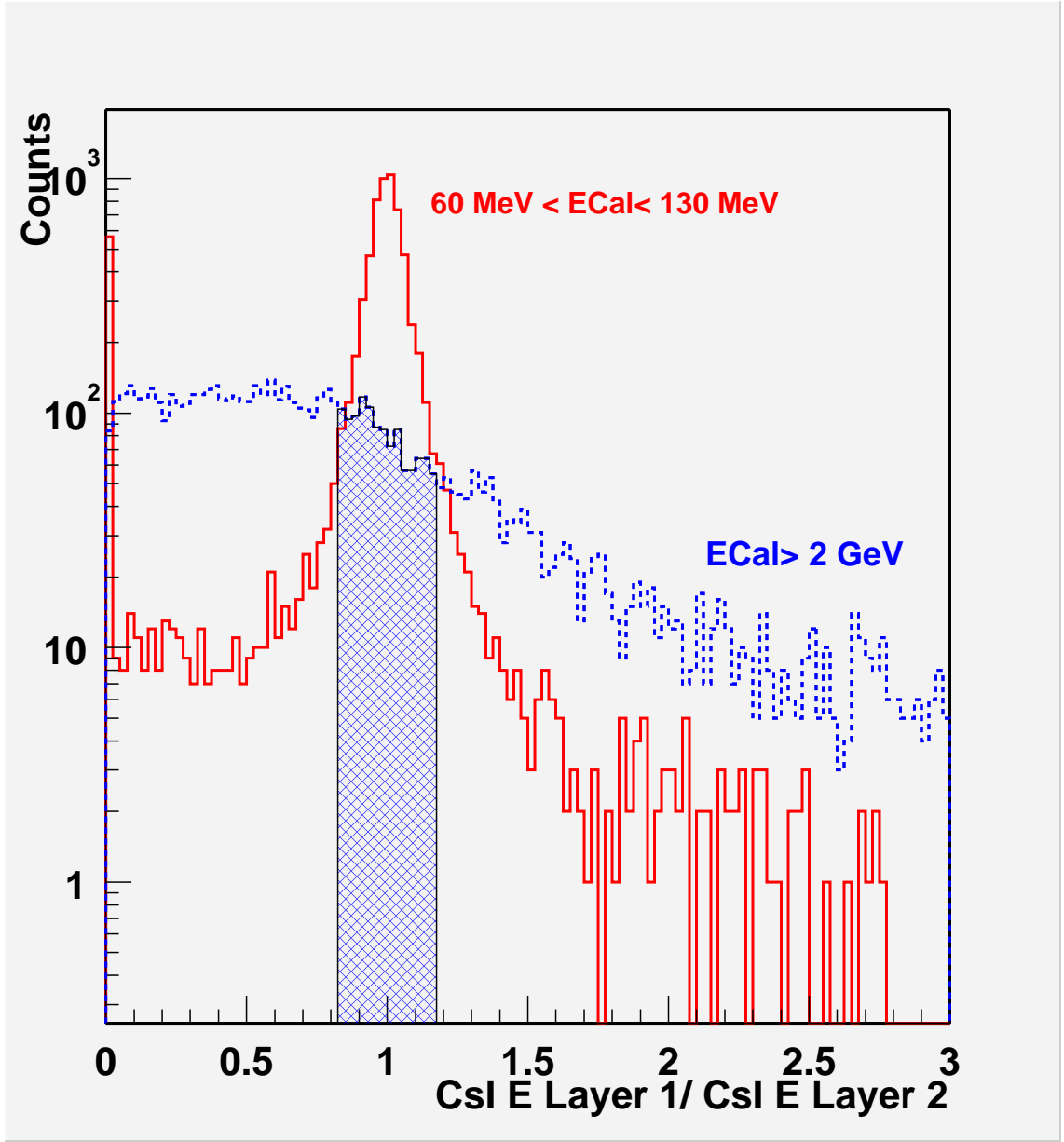


Figure 9: Distribution of the ratio of the energies deposited in the first and second crystal layers for two sets of events with different ECal. The hatched area corresponds to events with a ratio included between 0.85 and 1.15 for  $E_{\text{Cal}} > 2$  GeV.